

Unsteady numerical simulation of solar chimney power plant system with energy storage layer

Y. Zheng¹, T. Z. Ming^{*1}, Z. Zhou¹, X. F. Yu¹, H. Y. Wang¹, Y. Pan² and W. Liu¹

Numerical simulations were carried out to analyse the performance of the solar chimney power plant systems with energy storage layer in this paper. Mathematical models were developed to describe the flow and heat transfer mechanisms of the collector, chimney and the energy storage layer, and the responses of different energy storage materials to the solar radiation, and the effects of these materials on the power output with different solar radiations were analysed. Numerical simulation results show the following: first, soil and gravel both have suitable values of the property of thermal inertia, and they could be used as energy storage material for the solar chimney system; second, energy storage layer with comparatively higher heat capacity can store more energy on sunny days and can thus effectively decrease the variations of the chimney outlet parameters caused by the fluctuations in solar radiation related to the day–night cycle; third, the higher the temperature of the energy storage layer surface, the larger the energy and the exergy loss from the solar chimney systems will be.

Keywords: Solar chimney power plant, Collector, Energy storage layer, Chimney

List of symbols

A	collector area, m^2
c	constant
c_p	specific heat, $\text{kJ kg}^{-1} \text{K}^{-1}$
d_b	particle diameter of the porous layer, m
F	inertia coefficient of the porous layer
g	gravitational acceleration, m s^{-2}
h	convection heat transfer coefficient, $\text{W m}^{-2} \text{K}^{-1}$
K	permeability of the porous media
p	pressure, Pa
Pr	Prandtl number
t	time, s
T	temperature, K
u	velocity, m s^{-1}
v	velocity, m s^{-1}
α	thermal diffusivity; absorptance of the collector canopy to the solar radiation energy
β	thermal expansion coefficient, K^{-1}
Δ	difference
ε	emissivity of the body surface
ϕ	heat transfer rate, W
φ	porosity
λ	thermal conductivity, W m^{-1}

μ	dynamic viscosity, $\text{kg m}^{-1} \text{s}^{-1}$
ρ	density of the material, kg m^{-3}
σ	turbulent Prandtl numbers for T , κ and ε ; Stefan–Boltzmann constant
τ	transmissivity of the body

Subscripts

a	air inside the collector
c	canopy
chim	chimney
down	bottom of the energy storage layer
e	environment
m	apparent value of the energy storage layer
s	solid matrix of the energy storage layer; surface of the energy storage layer
w	wall of the chimney

Introduction

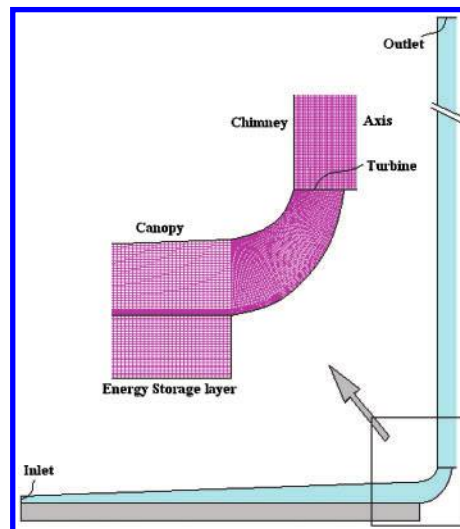
The solar chimney (SC) power plant system was first proposed in the late 1970s by Professor J. Schlaich and tested with a prototype model in Manzanares, Spain, in the early 1980s.^{1,2} Compared with the traditional power generation systems, the system has the following advantages: easier to design, more convenient to draw materials, higher operational reliability, fewer running components, more convenient maintenance and overhaul and lower maintenance expense, no environmental contamination, continuous stable running and longer operational life span. It has the potential to meet the power needs of developing countries and territories,

¹School of Energy and Power Engineering, Huazhong University of Science and Technology, Wuhan 430074, China
²College of Electrical and Electronic Engineering, Huazhong University of Science and Technology, Wuhan 430074, China

*Corresponding author, email mtzhen@163.com

especially in deserts where electric power is in shortage, with extensive prospect of application.

As the SC systems could make significant contributions to the energy supplies of those countries where there is plenty of desert land, which is not being utilised, in recent years, many researchers have made research reports on this technology and have carried out tracking study on SC systems. Pasumarthi and Sherif^{3,4} developed a mathematical model to study the effects of various environment conditions and geometry on the flow and heat transfer characteristics and output power of the SC, and they also developed three different models in Florida and reported the experimental data to assess the viability of the SC concept. Lodhi⁵ presented a comprehensive analysis of the chimney effect, power production and efficiency, and estimated the cost of the SC set-up in developing nations. Bernardes *et al.*⁶ presented a theoretical analysis of an SC, operating on natural laminar convection under steady state. Gannon and von Backström⁷ presented an air standard cycle analysis of the SC for the calculation of limiting performance, efficiency and relationship among main variables, including chimney friction, system, turbine and exit kinetic energy losses. Gannon and von Backström⁸ presented an experimental investigation of the performance of an SC turbine. The measured results showed that the SC turbine presented has a total/total efficiency of 85–90% and total/static of 77–80% over the design range. Later, the same authors⁹ presented analytical equations in terms of turbine flow and load coefficient and degree of reaction, to express the influence of each coefficient on turbine efficiency. Bernardes *et al.*¹⁰ established a rounded mathematical model for SC system on the basis of energy balance principle. Pastohr *et al.*¹¹ carried out a two-dimensional (2D) steady state numerical simulation study on the whole SC system, which consists of energy storage layer, collector, turbine and the chimney, and obtained the distributions of velocity, pressure and temperature inside the collector. Schlaich and Weinrebe¹² made an analysis on the operation principle of SC system and predicted the commercial application prospect of large scale SC system. Ming *et al.*¹³ developed a comprehensive model to evaluate the performance of an SC system, in which the effects of various parameters on the relative static pressure, driving force, power output and efficiency have been further investigated. Pretorius and Kröger¹⁴ evaluated the influence of a developed convective heat transfer equation, more accurate turbine inlet loss coefficient, quality collector roof glass and various types of soil on the performance of a large scale SC system. Bilgen and Rheault¹⁵ designed an SC system for power production at high latitudes and evaluated its performance. Koonsrisuk and Chitsomboon¹⁶ proposed dimensionless variables to guide the experimental study of flow in a small scale SC and employed a computational fluid dynamics methodology to explore the results that were used to prove the similarity of the proposed dimensionless variables. Maia *et al.*^{17,18} and Ferreira *et al.*¹⁹ gave detailed theoretical evaluations of the influence of geometric parameters and materials on the behaviour of the airflow in an SC prototype and analysed the airflow characteristics of the systems, which can be used as dryer for agriculture. Ming *et al.*²⁰ carried out numerical simulations on the SC



1 Physical model of SC prototype

systems coupled with a three-blade turbine using the Spanish prototype as a practical example and presented design and simulation of a megawatt graded SC system with a five blade turbine, the results of which show that the coupling of turbine increases the maximum power output of the system and the turbine efficiency is also relatively rather high. Ming *et al.*²¹ established different mathematical models for the collector, the chimney and the energy storage layer and analysed the effect of solar radiation on the heat storage characteristic of the energy storage layer. Zhou *et al.*^{22,23} presented some experimental and numerical results of a pilot SC equipment. Ming *et al.*²⁴ presented a simple analysis on the thermal performance of SC power generation systems.

The energy storage layer, without which the whole system could not operate continuously during the night, undoubtedly plays a significant role in the power output of a SC system. Part of the solar radiation is absorbed by the energy storage layer during the daytime and is released during the nights or days with cloudy weather. Pastohr *et al.*¹¹ presented a numerical simulation result in which the energy storage layer was regarded as solid. The energy storage layer, however, can be treated as porous media, as there is air flowing inside the solid matrix, especially when the SC systems are built in Gobi or in the desert land in the northwest of China with energy storage layer made of gravel or sand. In this article, unsteady conjugate numerical simulations of the SC system with the energy storage layer, the collector and the chimney were carried out. However, it is not necessary to take the turbine into consideration for a 2D axisymmetric flow, as the 2D turbine can only describe the flow and heat transfer characteristics of the system with an ideal pressure drop at a certain place. In addition, the effect of the heat storage characteristic of the energy storage layer on the air flow and heat transfer characteristics of the system is also taken into consideration.

Numerical models

System description

The physical model of the Spanish SC power generating system prototype shown in Fig. 1 (Ref. 11) is selected as a physical model for the numerical simulation. The

prototype has a chimney with 200 m height and 5 m radius and a collector with 122 m radius and 2 m height. The solid matrix of the energy storage layer is soil or gravel with large heat capacity.

However, the analysis described in this paper should be based on some simple assumptions shown as follows. First, axisymmetric flow of air in the collector is assumed, i.e. non-uniform heating of the collector surface in terms of the sun's altitude angle is neglected. Second, an average value for the optical properties is considered to estimate the radiation incident on the absorber surface. Therefore, the transmittance of beam radiation during early sunshine hours would be considerably lower than the average value of the transmittance. Third, the Boussinesq approximation is assumed to be valid. This approximation neglects all variation of properties except for density in the momentum equation. Fourth, the solar radiation is thought to be transient with time, but the ambient temperature and wind speed are assumed constant. This assumption is advanced only considering that it is a little difficult to get a convergent simulation result if the ambient parameters were set to be transient with time.

Theoretical modelling

The continuity equation, Navier–Stokes equation, energy equation and κ – ε equations can be used to describe the air flow and heat transfer in the collector and chimney shown as follows

$$\frac{\partial \rho}{\partial t} + \frac{\partial(\rho u)}{\partial x} + \frac{1}{r} \frac{\partial(\rho v)}{\partial r} = 0 \tag{1}$$

$$\frac{\partial(\rho u)}{\partial t} + \frac{\partial(\rho uu)}{\partial x} + \frac{1}{r} \frac{\partial(\rho rvu)}{\partial r} = \rho g \beta (T - T_\infty) + \frac{\partial}{\partial x} \left[(\mu + \mu_t) \frac{\partial u}{\partial x} \right] + \frac{1}{r} \frac{\partial}{\partial r} \left[(\mu + \mu_t) r \frac{\partial u}{\partial r} \right] \tag{2}$$

$$\frac{\partial(\rho v)}{\partial t} + \frac{\partial(\rho uv)}{\partial x} + \frac{1}{r} \frac{\partial(\rho rvv)}{\partial r} = \frac{\partial}{\partial x} \left[(\mu + \mu_t) \frac{\partial v}{\partial x} \right] + \frac{1}{r} \frac{\partial}{\partial r} \left[(\mu + \mu_t) r \frac{\partial v}{\partial r} \right] \tag{3}$$

$$\frac{\partial(\rho T)}{\partial t} + \frac{\partial(\rho u T)}{\partial x} + \frac{1}{r} \frac{\partial(\rho v T)}{\partial r} = \frac{\partial}{\partial x} \left[\left(\frac{\mu}{Pr} + \frac{\mu_t}{\sigma_T} \right) \frac{\partial T}{\partial x} \right] + \frac{1}{r} \frac{\partial}{\partial r} \left[r \left(\frac{\mu}{Pr} + \frac{\mu_t}{\sigma_T} \right) \frac{\partial T}{\partial r} \right] \tag{4}$$

$$\frac{\partial(\rho \kappa)}{\partial t} + \frac{\partial(\rho \kappa u)}{\partial x} + \frac{1}{r} \frac{\partial(\rho r v \kappa)}{\partial r} = \frac{\partial}{\partial x} \left[\left(\mu + \frac{\mu_t}{\sigma_\kappa} \right) \frac{\partial \kappa}{\partial x} \right] + \frac{1}{r} \frac{\partial}{\partial r} \left[\left(\mu + \frac{\mu_t}{\sigma_\kappa} \right) r \frac{\partial \kappa}{\partial r} \right] + G_\kappa - \rho \varepsilon \tag{5}$$

$$\frac{\partial(\rho \varepsilon)}{\partial t} + \frac{\partial(\rho \varepsilon u)}{\partial x} + \frac{1}{r} \frac{\partial(\rho r v \varepsilon)}{\partial r} = \frac{\partial}{\partial x} \left[\left(\mu + \frac{\mu_t}{\sigma_\varepsilon} \right) \frac{\partial \varepsilon}{\partial x} \right] + \frac{1}{r} \frac{\partial}{\partial r} \left[\left(\mu + \frac{\mu_t}{\sigma_\varepsilon} \right) r \frac{\partial \varepsilon}{\partial r} \right] + \frac{\varepsilon}{\kappa} (c_1 G_\kappa - c_2 \rho \varepsilon) \tag{6}$$

where, G_κ represents the generation of turbulence kinetic energy due to the mean velocity gradients defined as

$$G_\kappa = -\mu_t \left\{ 2 \left[\left(\frac{\partial u}{\partial x} \right)^2 + \left(\frac{\partial v}{\partial r} \right)^2 + \left(\frac{v}{r} \right)^2 \right] + \left(\frac{\partial u}{\partial r} + \frac{\partial v}{\partial x} \right)^2 \right\}$$

σ_T , σ_κ and σ_ε are the turbulent Prandtl numbers for T , κ and ε respectively, and c_1 and c_2 are two constants for turbulent model: $c_1=1.44$, $c_2=1.92$, $\sigma_T=0.9$, $\sigma_\kappa=1.0$, $\sigma_\varepsilon=1.3$, $\mu_t = c_\mu \rho \kappa^2 / \varepsilon$ and $c_\mu=0.09$.

The heat transfer and flow in the energy storage layer may be very complicated, and it is necessary to consider the collector, the chimney and the storage medium as a whole system. As the material used for energy storage can be regarded as porous media, the Brinkman–Forchheimer extended Darcy model²⁵ is used to describe the flow in the convective porous layer, which can be expressed as follows

$$\frac{\partial \rho}{\partial t} + \frac{\partial(\rho u)}{\partial x} + \frac{1}{r} \frac{\partial(\rho v)}{\partial r} = 0 \tag{7}$$

$$\begin{aligned} & \frac{1}{\varphi} \frac{\partial(\rho u)}{\partial t} + \frac{1}{\varphi^2} \left[\frac{\partial(\rho uu)}{\partial x} + \frac{1}{r} \frac{\partial(\rho rvu)}{\partial r} \right] \\ & = \rho g \beta (T - T_e) + \frac{\partial}{\partial x} \left(\mu_m \frac{\partial u}{\partial x} \right) + \frac{1}{r} \frac{\partial}{\partial r} \left(r \mu_m \frac{\partial u}{\partial r} \right) \\ & - \frac{\mu u}{K} - \frac{\rho F}{K^{1/2}} (u^2 + v^2)^{1/2} u \end{aligned} \tag{8}$$

$$\begin{aligned} & \frac{1}{\varphi} \frac{\partial(\rho v)}{\partial t} + \frac{1}{\varphi^2} \left[\frac{\partial(\rho uv)}{\partial x} + \frac{1}{r} \frac{\partial(\rho rvv)}{\partial r} \right] \\ & = \frac{\partial}{\partial x} \left(\mu_m \frac{\partial v}{\partial x} \right) + \frac{1}{r} \frac{\partial}{\partial r} \left(r \mu_m \frac{\partial v}{\partial r} \right) - \mu_m \frac{v}{r^2} \\ & - \frac{\mu v}{K} - \frac{\rho F}{K^{1/2}} (u^2 + v^2)^{1/2} v \end{aligned} \tag{9}$$

$$\begin{aligned} & \rho_m c_{p,m} \left[\frac{\partial T}{\partial t} + \frac{\partial(uT)}{\partial x} + \frac{1}{r} \frac{\partial(rvT)}{\partial r} \right] \\ & = \frac{\partial}{\partial z} \left(\lambda_m \frac{\partial T}{\partial x} \right) + \frac{1}{r} \frac{\partial}{\partial r} \left(r \lambda_m \frac{\partial T}{\partial r} \right) \end{aligned} \tag{10}$$

where φ , ρ_m , $c_{p,m}$, μ_m and λ_m are the porosity, apparent density, specific capacity, dynamic viscosity and apparent thermal conductivity of the porous medium respectively: $\rho_m=(1-\varphi)\rho_s + \varphi\rho_a$, $c_{p,m}=(1-\varphi)c_{p,s} + \varphi c_{p,a}$, $\lambda_m=(1-\varphi)\lambda_s + \varphi\lambda_a$ and $\mu_m=\mu\varphi$, the parameters with subscripts s and a denote the corresponding parameters of the solid and air in the energy storage layer respectively. K , F and d_b are the permeability, the inertia coefficient and the particle diameter of the energy storage layer respectively.

$$K = \frac{d_b^2 \varphi^3}{175(1-\varphi)^2} \tag{11}$$

$$F = \frac{1.75\varphi^{-1.5}}{175^{1/2}} \tag{12}$$

Boundary conditions and initial conditions

Boundary conditions for side faces of energy storage layer

$$\left. \frac{\partial T}{\partial r} \right|_{r=R} = 0, \quad u=0, \quad v=0 \tag{13}$$

There might be a heat transfer phenomenon between the outside face of the energy storage layer and the material nearby. Thereby, a simplification of this boundary as shown in equation (13) may overestimate the local temperature profile of the energy storage layer near this place.

Boundary conditions for chimney wall

The boundary conditions for the chimney wall can be shown as

$$\left. \frac{\partial T}{\partial r} \right|_w = 0, \quad u=0, \quad v=0 \quad (14)$$

Boundary conditions for collector inlet and chimney outlet

According to the analysis by Pastohr *et al.*,¹¹ the static pressure difference Δp between the collector inlet and the environment at the same height is 0 Pa, and temperature approximately equals the environment temperature. In addition, the boundary condition for the chimney outlet should be pressure outlet, and the pressure at this place should also be equal to that of the environment with the same height

$$\Delta p_{\text{inlet}} = 0, \quad T_{\text{inlet}} = T_e \quad (15)$$

Similar to the method applied by Pastohr *et al.*,¹¹ the absorption of the solar radiation is considered as a source term in the energy storage layer with a thickness of 0.1 mm. In addition, the boundary condition for the bottom of the energy storage layer could be selected as constant temperature condition, as the temperature distribution 5 m below the surface varies slightly. The boundary conditions for the SC system are shown in Ref. 24.

Initial conditions

It can be easily seen from the boundary conditions shown above that ϕ_{solar} will change with time during a day. Thereby, the solar radiation, the air temperature in the environment and the initial conditions of the system should be given as follows to analyse the unsteady heat transfer and flow characteristics of the SC system

$$t=0, \quad T_e = \text{constant}, \quad u=0, \quad v=0 \quad (16)$$

$$\phi_{\text{solar}} = \phi_{\text{solar,max}} \sin\left(\frac{t-1440n}{720}\pi\right) \quad (17)$$

$$0 \leq t-1440n < 720 \quad (n=0,1, \dots, 4)$$

$$\phi_{\text{solar}} = 0 \quad 720 \leq t-1440n < 1440 \quad (n=0, 1, \dots, 4) \quad (18)$$

where n is the ordinal number of the sunny days, which varies from 0 to 4, and $\phi_{\text{solar,max}}$ is the maximum value of the solar radiation including the beam radiation, diffuse sky radiation and ground reflected radiation.

Solution method

For the present study, the governing equations (1)–(6) and (7)–(10) together with all the boundary conditions and initial conditions mentioned above equations (13)–(18) were solved with the SIMPLE method using the commercial software FLUENT 6.3. Standard $k-\epsilon$ model was used to describe the flow and heat transfer inside the collector and chimney, and the Brinkman–

Forchheimer extended Darcy model was used to describe the flow and heat transfer in the energy storage layer. QUICK format was used to the discretisation of the momentum, energy and other equations. The non-uniform mesh sizes were used for the numerical computation. For one physical model, we got the grid independent solution if the grids are ~ 1.0 million, thereby the grids of the SC power plant in these simulations are ~ 1.1 million, which is acceptable to get reliable results.

During the simulation process, $\phi_{\text{solar,max}}$ and T_e are 1000 W m^{-2} and 293 K respectively. The temperature of the bottom of the energy storage layer is preset as 300 K for a physical model built in Wuhan, one of the three most sweltering cities in China. The two materials used to analyse the effect of the energy storage layer on performance of the SC system are soil and gravel. The properties of the soil are as follows: $\rho_{\text{soil}}=1700 \text{ kg m}^{-3}$, $c_{p,\text{soil}}=2016 \text{ J kg}^{-1} \text{ K}^{-1}$ and $\lambda_{\text{soil}}=0.78 \text{ W m}^{-1} \text{ K}^{-1}$. The properties of the gravel are $\rho_{\text{gravel}}=2555 \text{ kg m}^{-3}$, $c_{p,\text{gravel}}=814.8 \text{ J kg}^{-1} \text{ K}^{-1}$ and $\lambda_{\text{gravel}}=2.00 \text{ W m}^{-1} \text{ K}^{-1}$. The absorptance of the energy storage layer surface is 0.9, and the porosities of the energy storage layers composed of soil and gravel are both selected as 0.3. The particle diameter of the soil and gravel are 0.5 and 4 cm respectively, and the time step is 5 min.

Reliability of simulation method

In order to confirm the reliability of the numerical simulation carried out in this paper, a comparison between the experimental results of the SC power plant prototype in Spain and the simulation results is necessary and is carried out as follows. Some parameters of the SC power plant prototype in Spain are set as follows: solar radiation, 1040 W m^{-2} ; absorptance of the ground, 0.56–0.67; permeability of the collector, 0.8 and ambient temperature, 303 K . When soil thickness is within 0–5 cm, the average thermal conductivity is $\sim 0.7 \text{ W m}^{-1} \text{ K}^{-1}$; when soil thickness is within 5–10 cm, the average thermal conductivity is $\sim 1.2 \text{ W m}^{-1} \text{ K}^{-1}$; when soil thickness is within 10–15 cm, the average thermal conductivity is $\sim 1.5 \text{ W m}^{-1} \text{ K}^{-1}$.

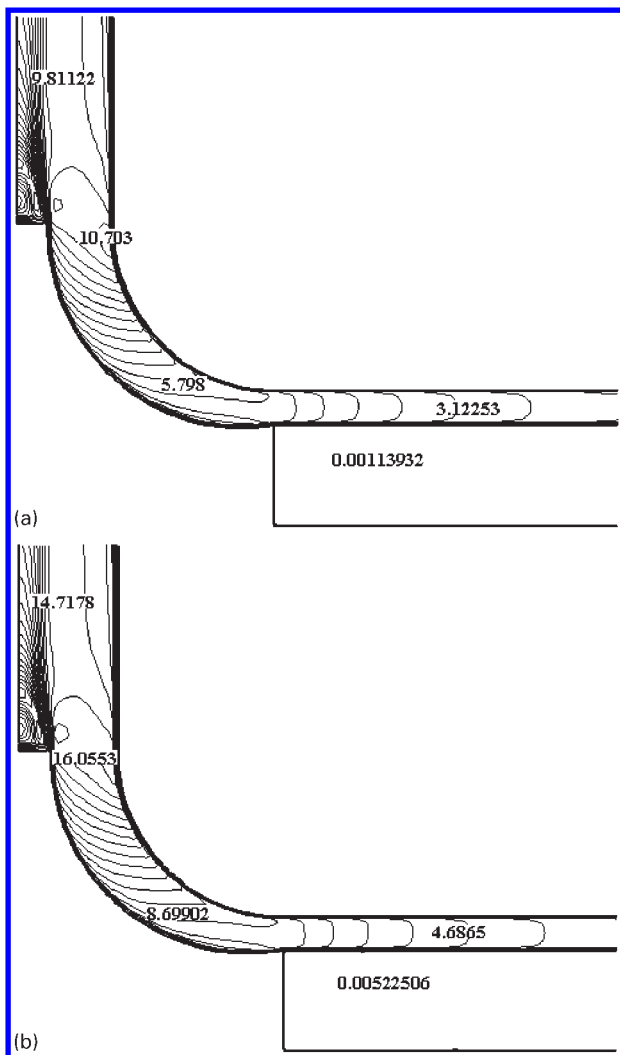
The comparison between the measured and numerical simulation results is shown in Table 1. It can be easily seen that the numerical simulation results agree well with the measured results, which indicate that the simulation method applied in this paper is reliable. The cause for the errors listed in Table 1 is the uncertainty of specific parameters, such as the density of gasoloid in the air, air humidity, optical parameters and the property parameters.

Results and discussion

One of the most attractive advantages of the SC systems is the continuous electricity supply regardless of the weather conditions and day–night cycle, and the cardinal part of

Table 1 Comparison between measured and simulated results

Parameters	Measured ²	Simulated	Error, %
Temperature rise of air, K	25	25.26645	1.0658
Velocity of air at the chimney inlet, m s^{-1}	9	8.812802	–2.079
Output power, kW	41	40.196	–1.96

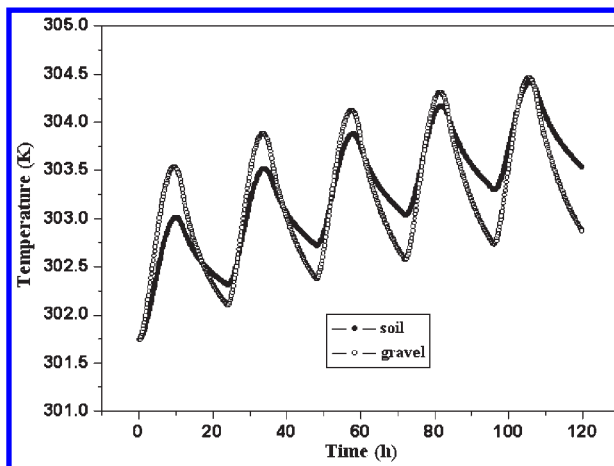


a solar radiation 200 W m^{-2} ; b solar radiation 800 W m^{-2}

2 Velocity distributions of the system under different solar radiation, m s^{-1}

the system to realise this advantage is the energy storage layer. The thermal performance of the energy storage layer plays an important role in the power output of the SC system with time. It is clear that the power output of the system is affected by the chimney inlet velocity, which is nearly equal to the chimney outlet velocity, while the surface temperature of the energy storage layer has significant influence on the air velocity of the chimney inlet, and the average temperature of the whole energy storage layer also notably affects the power output of the system especially when there is no solar radiation at night or on cloudy days. Hence, a detailed description should be given on the temperature distribution of the system and the air velocity of the chimney outlet with the variation of solar radiation.

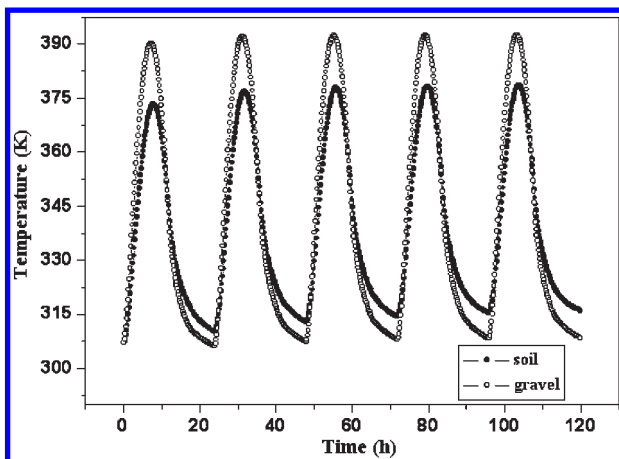
Figure 2 gives a description of the velocity distributions of the SC system with energy storage layer, which is made of soil. It can be seen from this figure that the velocity inside the collector and chimney is about several metres per second, while it is rather small inside the energy storage layer, and the air velocity of the whole system increases with the solar radiation, where the maximum velocity lies at the bottom of the tower. Simulation results indicate that the temperature inside



3 Variations of bulk temperature of different energy storage layers with time

the chimney is only 304 K when the solar radiation is 200 W m^{-2} , while it reaches 321 K when the solar radiation is 800 W m^{-2} , which show that solar radiation has significant influence on the air temperature of the chimney. Further results of numerical simulation with a certain solar radiation and comparison of different models can be found in Ref. 21.

Figure 3 shows the variations of bulk temperature of different energy storage layers with time, where 0 of the abscissa is 06:00 of the first day. From the figure, it can be seen that the bulk temperature of the gravel energy storage layer changes more notably than that of the soil energy storage layer during the 5 days. For a given day, the change scope of bulk temperature of the gravel system is $\sim 1 \text{ K}$, which is nearly 80% larger than that of the soil system. This is because the heat capacity of soil is much higher than that of gravel; therefore, the temperature of the gravel energy storage layer changes more notably than that of the soil energy storage layer. As time goes on, the maximum temperature of the soil energy storage layer gradually reaches that of the gravel energy storage layer, and the difference is very small on the fifth day. On the contrary, the difference of the minimum temperature between the two types of energy storage layer becomes more and more notable. For the soil energy storage layer, the temperature difference between the day and night decreases gradually; this is because the energy storage increases, and the temperature of the energy storage layer will not decrease significantly even though large amount of heat energy dissipates from the energy storage layer during the night. In addition, there is a lag effect on the solar radiation for the maximum and minimum temperature of different types of energy storage layer. For the first day, the maximum temperature of the energy storage layer occurs at about 16:00, and the minimum temperature occurs at about 04:00 the next day, but these values come comparatively later in the subsequent days. This phenomenon shows that the energy storage layer has the thermal inertia characteristic and has a very notable effect on energy storage. In addition, the overall trend of the bulk temperature seems to increase continuously and show no sign of stabilisation. The reason is that for a 5 m energy storage layer, simulation with 5 days of energy storage is not enough, only when the energy released is equal to the energy storage will the numerical results stabilise.



4 Variations of surface temperature of energy storage layers with time

The variations of the surface temperature of the energy storage layer with time are shown in Fig. 4. From this figure, it can be seen that there is a more notable variation of the surface temperature of the gravel energy storage layer than that of the soil energy storage layer. By comparison, the maximum temperature of the gravel energy storage layer is 15 K higher than that of the soil energy storage layer, while the minimum temperature of the former is 2 K lower than that of the latter.

The surface temperature of the energy storage layer has a very significant effect on the performance of the SC system. Heat transfer is an irreversible process accompanied with exergy loss to some extent. The higher the surface temperature of the energy storage layer, the larger the temperature difference between the energy storage layer surface and the air inside the collector, and the larger the extent of irreversibility of the heat transfer process, which results in a larger entropy generation. According to the definition of exergy loss, which is the product of environment temperature and entropy generation, the exergy loss caused by the heat transfer process from the higher temperature of the surface of the energy storage layer to the air inside the collector is comparatively larger, and the collector efficiency therefore decreases. As a result, as shown in Fig. 4, the extent of irreversibility caused by heat transfer process using the soil energy storage layer is less than that using the gravel energy storage layer, with a comparatively lower exergy loss. This is very beneficial for the increase in the power output efficiency of the SC system. In addition, the higher the surface temperature of the energy storage layer, if we look inside the temperature gradient of the energy storage layer with a constant temperature of the bottom of the energy storage layer, the larger the temperature difference between the surface and the bottom of the energy storage layer, the greater the temperature gradient inside and the larger the energy loss from the bottom of the energy storage layer to the deeper soil, which could never be used again by the SC system. On the other hand, a comparatively larger temperature gradient inside the energy storage layer will also result in larger exergy loss from the system.

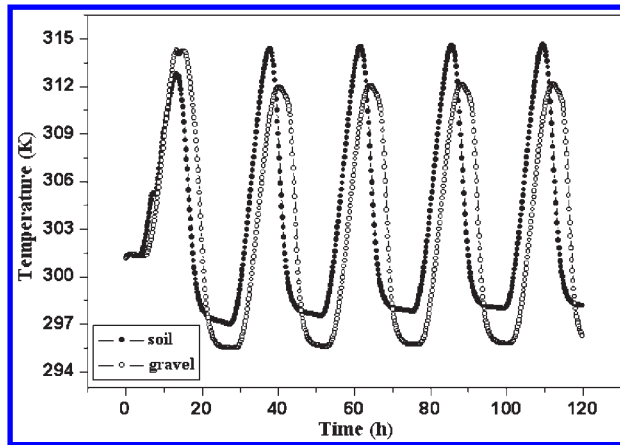
Hence, the effects of the surface temperature of the energy storage layer on the SC systems could be described at least in two aspects: first, the higher the surface temperature of the energy storage layer, the larger the energy loss from the bottom of the energy storage layer

based on the first law of thermodynamics; second, the higher the surface temperature of the energy storage layer, based on the second law of thermodynamics, the higher the extent of irreversibility during the heat transfer process both inside the energy storage layer and from the energy storage layer surface to the air inside the collector and the larger the exergy loss during the energy transfer process. Therefore, in order to decrease the energy and exergy loss and also to increase the efficiency of the SC system, it is a very effective approach to decrease the surface temperature of the energy storage layer.

There are several methods shown as follows, to decrease the surface temperature of the energy storage layer. In the first way, a material with high heat capacity could be selected as the energy storage medium, which could decrease the surface temperature of the energy storage layer effectively. It is thus an effective way to pave water pipes on the ground inside the collector instead of other energy storage material, since there may be a large amount of energy stored in the water without large temperature difference for the SC system. In the second place, applying material with comparatively larger thermal conductivity as energy storage medium can also decrease the surface temperature of the energy storage layer. With the same heat transfer rate, the temperature difference is smaller in the material whose thermal conductivity is higher, and it is therefore useful to adopt a composite energy storage layer with the upper using higher thermal conductivity material and the nether using comparatively lower thermal conductivity, as this kind of energy storage layer could decrease the surface temperature of the energy storage layer with comparatively smaller amount of energy loss from the bottom to the deeper soil. In addition, different kinds of plants, such as flowers and vegetables, could be cultivated at different places inside the collector, which can improve the air quality and humidity and also decrease the surface temperature of the energy storage layer.

Figures 5 and 6 show the variations of the chimney outlet parameters with time. Air flows inside the collector absorbing energy from the surface of the energy storage layer, and the amount of energy absorbed has an effect on the air temperature and velocity. The larger the amount of energy absorbed by the air, the higher the air temperature and velocity of the airflow of the chimney outlet, while the lower the amount of energy absorbed by the air, the lower the air temperature and velocity of the chimney outlet. When soil is selected as the energy storage medium, the daytime temperature and velocity of the airflow of the chimney outlet from 05:00 to 21:00 will be higher than that when gravel is selected. The temperature and velocity of the outlet at night from 21:00 to 05:00 will be lower for soil than for gravel. The reason is that the thermal conductivity of soil is lower than that of gravel, which results in a comparatively higher temperature difference between the energy storage layer surface and the air inside the collector under the same solar radiation; this creates a comparatively higher heat transfer rate between the energy storage layer surface and the air, where the heat transfer coefficient corresponds to the air velocity, which increases with the increasing the temperature difference between the energy storage layer surface and the air.

The energy storage layer, which can absorb and store solar energy during sunny days while releases heat energy to



5 Variations of chimney outlet temperature with time

the air inside the collector at nights or in rainy and cloudy days, plays an important role in the continuous fluid flow, heat transfer and power output of the SC system. Another aim of the energy storage layer is to decrease the system power output difference between the day and night by decreasing the variations of the chimney outlet parameters, especially air velocity. If the variations are too large, the variation of power output of the SC with time will be very large. It can be seen from Figs. 5 and 6 that the variation scales of the chimney outlet parameters with time are very large; a possible method to decrease these differences is to replace soil and gravel with a kind of energy storage layer made of a new type of composite material whose thermal conductivity decreases as temperature increases, and another possible method is to use a kind of material whose thermal conductivity is higher than that of the gravel but lower than that of the soil. Therefore, heat conduction of the energy storage layer has a complicated effect on the power output characteristic of the SC system. A comparatively higher heat conduction of the energy storage layer will decrease the surface temperature of the energy storage layer, which will result in the decreases in energy and exergy loss from the system. On the other hand, a higher heat conduction of the energy storage layer will decrease the heat transfer resistance between the surface of the energy storage layer and the air inside the collector. Hence, care must be taken with the thermal conductivity and heat capacity of the energy storage layer for the power output performance of the SC systems.

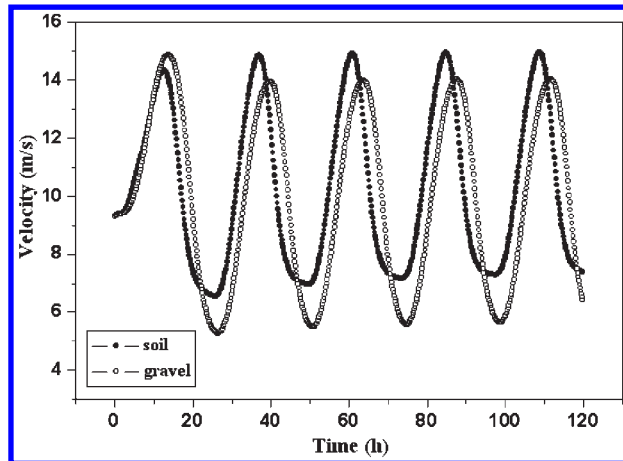
Further study will consider the effects of the absorptivity and absorptivity of the canopy, and the porosity of the energy storage layer on the performance of the SC system. In addition, research on the performance of SC system by changing both the turbine pressure drop and the solar radiation is also valuable.

Conclusions

Unsteady numerical simulations on the SC system with energy storage layer were carried out, and the energy storage layer was regarded as porous medium. Numerical simulation results show the following:

1. Soil and gravel both have suitable values of the property of thermal inertia, and they could be used as energy storage material for the SC system.

2. When energy storage layer with larger heat capacity is adopted, a larger part of energy from solar



6 Variations of chimney outlet velocity with time

radiation on sunny days can be stored inside the energy storage layer and released at night or on cloudy days.

3. The fluctuations in the chimney outlet velocity, temperature and the bulk temperature of the energy storage layer will also decrease when energy storage layer with larger heat capacity is adopted.

References

1. W. Haaf, K. Friedrich, G. Mayer and J. Schlaich: *Int. J. Solar Energy*, 1983, **2**, 3–20.
2. W. Haaf: *Int. J. Solar Energy*, 1984, **2**, 141–161.
3. N. Pasumarthi and S. A. Sherif: *Int. J. Energy Res.*, 1998, **22**, 277–288.
4. N. Pasumarthi and S. A. Sherif: *Int. J. Energy Res.*, 1998, **22**, 443–461.
5. M. A. K. Lodhi: *Energy Convers. Manage.*, 1999, **40**, 407–421.
6. M. A. D. S. Bernardes, R. M. Valle and M. F. B. Cortez: *Int. J. Therm. Sci.*, 1999, **38**, 42–50.
7. A. J. Gannon and T. W. von Backström: *J. Solar Energy Eng.*, 2000, **122**, 133–137.
8. A. J. Gannon and T. W. von Backström: *J. Solar Energy Eng.*, 2003, **125**, 101–106.
9. T. W. von Backström and A. J. Gannon: *Solar Energy*, 2004, **76**, 235–241.
10. M. A. D. S. Bernardes, A. Vob and G. Weinrebe: *Solar Energy*, 2003, **75**, 511–524.
11. H. Pastohr, O. Kornadt and K. Gurlebeck: *Int. J. Energy Res.*, 2004, **28**, 495–510.
12. J. Schlaich and G. Weinrebe: *J. Solar Energy Eng.*, 2005, **127**, 117–124.
13. T. Z. Ming, W. Liu and G. L. Xu: *Int. J. Energy Res.*, 2006, **30**, 861–873.
14. J. P. Pretorius and D. G. Kröger: *Solar Energy*, 2006, **80**, 535–544.
15. E. Bilgen and J. Rheault: *Solar Energy*, 2006, **79**, 449–458.
16. A. Koonsrisuk and T. Chitsomboon: *Solar Energy*, 2007, **81**, 1439–1446.
17. C. B. Maia, A. G. Ferreira, R. M. Valle and M. F. B. Cortez: *Comput. Fluids*, 2009, **38**, 625–636.
18. C. B. Maia, A. G. Ferreira, R. M. Valle and M. F. B. Cortez: *Heat Transfer Eng.*, 2009, **30**, 393–399.
19. A. G. Ferreira, C. B. Maia, M. F. B. Cortez and R. M. Valle: *Solar Energy*, 2008, **82**, 198–205.
20. T. Z. Ming, W. Liu, G. L. Xu, Y. Xiong, X. Guan and Y. Pan: *Renew. Energy*, 2008, **33**, 897–905.
21. T. Z. Ming, W. Liu, Y. Pan and G. Xu: *Energy Convers. Manage.*, 2008, **49**, 2872–2879.
22. X. P. Zhou, J. K. Yang, B. Xiao and F. Long: *J. Energy Inst.*, 2008, **81**, 86–91.
23. X. P. Zhou and J. K. Yang: *J. Energy Inst.*, 2008, **81**, 25–30.
24. T. Z. Ming, Y. Zheng, C. Liu, W. Liu and Y. Pan: *J. Energy Inst.*, 2010, **83**, 6–11.
25. J. K. Sung and Y. C. Christopher: *Int. J. Heat Mass Transfer*, 1996, **39**, 319–329.